

Non-threaded isomers of sungsanpin and ulleungdin lasso peptides inhibit H1299 cancer cell migration

Lori Digal,¹ Shiela C. Samson,² Mark A. Stevens,¹ Abhijit Ghorai,¹ Hyungyu Kim,³ Marcus C. Mifflin,¹ Keith R. Carney,² David L. Williamson,¹ Soohyun Um,⁴ Gabe Nagy,¹ Dong-Chan Oh,³ Michelle C. Mendoza,² and Andrew G. Roberts*¹

¹ Department of Chemistry, University of Utah, 315 South 1400 East, Salt Lake City, Utah 84112, USA

² Huntsman Cancer Institute, Salt Lake City, UT 84112, USA.

³ Natural Products Research Institute, College of Pharmacy, Seoul National University, 1 Gwanak-ro, Gwanak-gu, Seoul 151-742, Republic of Korea

⁴ College of Pharmacy, Yonsei Institute of Pharmaceutical Sciences, Yonsei University, 85 Songdogwahak-ro, Incheon, 21983, Republic of Korea

Supporting Information Placeholder

ABSTRACT: Lasso peptides are a structurally distinct class of biologically active natural products, defined by their short sequences with impressively interlocked tertiary structures. Their characteristic peptide [1]rotaxane motif confers marked proteolytic and thermal resiliency, and reports on their diverse biological functions have been credited to their exceptional sequence variability. Because of these unique properties, taken together with improved technologies for their biosynthetic production, lasso peptides are emerging as a designable scaffold for peptide-based therapeutic discovery and development. Although the defined structure of lasso peptides is recognized for its remarkable properties, the role of the motif for imparting bioactivity is less understood. For example, sungsanpin and ulleungdin are natural lasso peptides that similarly exhibit encouraging cell migration inhibitory activities in A549 lung carcinoma epithelial cells despite sharing only one-third sequence homology. We hypothesized that the shape of the lasso motif is beneficial for the preorganization of the conserved residues, which might be partially retained in variants lacking the threaded structure. Herein, we describe solid-phase peptide synthesis strategies to prepare acyclic, head-to-sidechain (branched), and head-to-tail (macrocyclic) cyclic variants based on the sungsanpin (Sun) and ulleungdin (Uln) sequences. Proliferation assays and time-lapse cell motility imaging studies were used to evaluate the cell inhibitory properties of natural Sun compared alongside the synthetic Sun and Uln isomers. These studies demonstrate that the lasso motif is not a required feature to slow cancer cell migration, and more generally show that these non-threaded isomers can retain similar activity to the natural lasso peptide despite the differences in their overall structures.

Introduction

Due to their fascinatingly threaded structures, remarkable stability to proteolytic degradation, diverse biological activities (e.g., glucagon receptor antagonism, bacterial RNA polymerase (RNAP) inhibition, cancer cell migration/invasion inhibition), and promise as scaffolds that can be engineered to exhibit

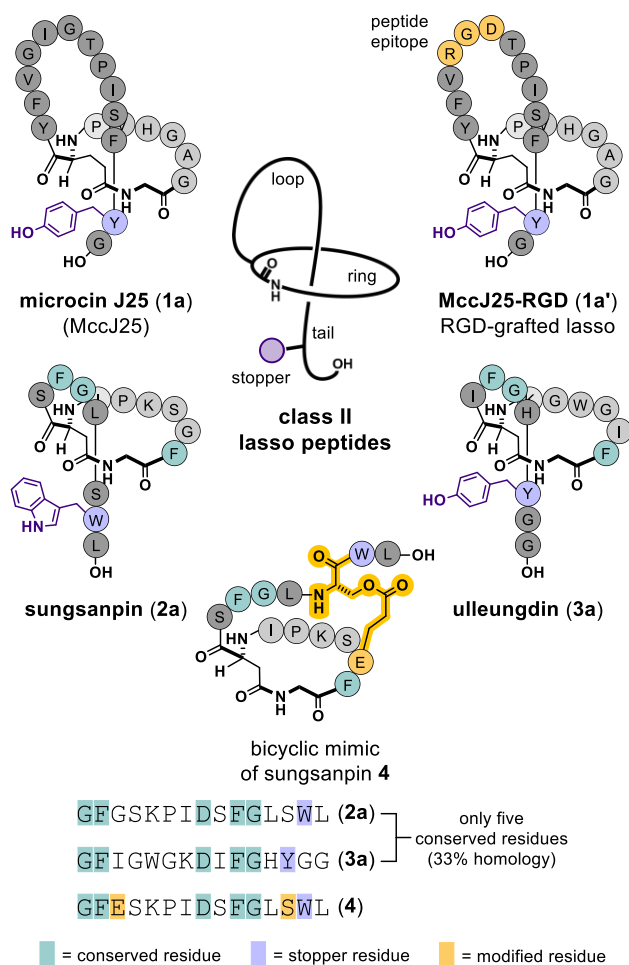


Figure 1. Bioactive class II lasso peptides inspire the development of stable cyclic peptides with novel functions. Sungsanpin and ulleungdin lasso peptides exhibit cell migration inhibitory activities in A549 lung carcinoma epithelial cells, suggesting their lasso motifs may be a less

critical recognition feature for their unknown mechanism(s) of action.

novel functions, lasso peptides have drawn considerable attention as structurally distinct ribosomally synthesized and post-translationally modified peptides (RiPPs).¹ Since their discovery, applied site-directed mutagenesis methods have curated sequence-diverse lasso peptide libraries to uncover trends that can help improve and diversify lasso peptide functions.² To accompany the surge of lasso peptide discovery efforts, *in silico* screening predictions and other bioinformatic approaches have been used to expedite the characterization of previously unknown lasso peptide biosynthetic gene clusters.³ As a result, the development of heterologous expression systems (*e.g.*, *E. coli*), the advent of lasso peptide cell-free biosynthesis, and residue-selective peptide modification strategies have enabled access to many natural and unnatural lasso peptide variants.⁴⁻⁷ Therapeutic discovery efforts have focused on the design of sequence-modified lasso peptides to improve and generate novel therapeutic modalities. For example, sequence mutations of the prototypical lasso peptide, microcin J25 **1a** (MccJ25), showed that ring-localized mutations can decrease bacterial RNAP inhibitory activity, while tail-localized mutations can impart an up to five-fold increase in the same activity (Fig. 1).² Moreover, Marahiel and coworkers showed that an RGD epitope grafted onto the native sequence loop (1a') of the inactive MccJ25 successfully converted it to a nanomolar integrin inhibitor.⁸

The promising potential of lasso peptides has led to considerable effort toward general access to these scaffolds through chemical synthesis—a challenge that has yet to be realized. Direct attempts to synthesize lasso peptides by the cyclization of their acyclic precursors have been unsuccessful, yielding only head-to-sidechain cyclic lasso peptide isomers. The only reported approach for accessing a native lasso peptide, the disulfide-containing BI-32169, incorporated a cryptand-imidazolium host-guest complex linked to side chains in the ring to template the key lasso-forming macrolactamization event.⁹ However, this elaborate strategy required sequence-dependent anchoring steps, thereby limiting its general adoption. As an alternative approach, the Bode and Evans groups have independently developed synthetic [1]rotaxanes utilizing cryptand-templated rings and peptide-based loops.¹⁰ Bode and coworkers showed that various peptide sequences can be grafted into the common rotaxane structure that importantly exhibited lasso peptide-like thermal and protease stabilities, which highlights their potential to serve as lasso peptide mimics.^{10a}

On the other hand, cases of non-threaded lasso peptide derivatives have been shown to possess varying levels of biological activity. Interestingly, head-to-sidechain **1b** and head-to-tail cyclic **1c** constitutional isomers (non-threaded) of natural MccJ25 do not exhibit bacterial RNAP inhibitory activities.¹¹ However, such drastic structural deviations are not always met with a loss of activity. Kaur and coworkers showed that disulfide-containing bicyclic and branched variants of the MccJ25 sequence, although reduced relative to the natural lasso, retained significant antibacterial activity against *S. Newport* despite being non-threaded sidechain-to-sidechain cyclic peptides.¹² Fliiss and coworkers compared the activity of similar cyclic disulfide MccJ25 variants against various Gram-negative and Gram-positive bacterial strains, demonstrating their ability to decrease bacterial RNAP activity.¹³ The beneficial role of this lasso motif can be seen in the crystal structure of MccJ25 bound within the secondary channel of RNAP determined Darst, Link, and coworkers.¹⁴ MccJ25 binds

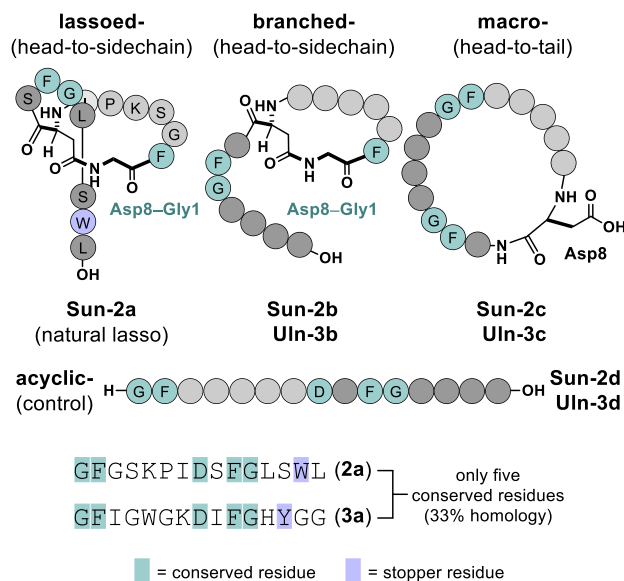


Figure 2. Motivating question: Is shape, the lasso motif, more important than sequence arrangement for the biochemical activities of sungsanpin and ulleungdin lasso peptides?

deep in this channel with the ring and tail facing the interior of the active site, which agrees with the effect of mutations on its activity. Still, carefully designed non-threaded peptides can RES-701-1, is a potent endothelin B receptor (ET_B) selective antagonist, whereas both the acyclic and head-to-sidechain isomers of RES-701-1 have significantly reduced binding activities.¹⁵ However, Yamasaki and coworkers showed that a head-to-sidechain hybrid peptide combining the ring segment of RES-701-1 with a C-terminal fragment of endothelin-1 gave improved ET_B binding activity, which improved further with the acyclic analog.¹⁶ The findings from these studies support future efforts to evaluate the properties of non-threaded acyclic and cyclic isomers of lasso peptides given their ease of access through chemical synthesis.

Cancer metastasis is a major cause of death in cancer patients that is initiated by migration of the cancer cells away from the primary tumor, and more efficacious treatments that inhibit this process are needed.¹⁷ Toward this end, we became interested in sungsanpin **2a** (isolated from *Streptomyces* sp. SNJ013) and ulleungdin **3a** (isolated from *Streptomyces* sp. KCB13F003), which exhibit similar cell migration inhibitory activities in A549 lung carcinoma epithelial cells despite sharing only one-third sequence homology.^{18,19} This observation suggests their similar lasso motifs may be a critical preorganization element for the conserved residues to impart their unknown mechanism(s) of action. We hypothesized that, while the lasso motif is beneficial, the arrangement of their sequence could be a more essential determinant for their activity. To examine this further, we designed a series of synthetically accessible sungsanpin (Sun-2b-2d) and ulleungdin (Uln-3b-3d) isomers to evaluate the spatial relationship of these sequences toward activity using time-lapse cell motility imaging assays with H1299 human non-small cell lung carcinoma cells. Specifically, we posited that partial conservation of the conserved sequence arrangement in these lasso peptides could bestow some comparable biological response across the series. The head-to-sidechain cyclic

isomers, Sun-**2b** and Uln-**3b**, were anticipated to be most like their respective threaded counterparts, sungsanpin **2a** and ulleungdin **3a**, whereas the acyclic peptides, Sun-**2d** and Uln-**3d**, were thought to have more disordered conformations and would therefore be the least active. Similarly, Tulla–Puche and coworkers prepared a sungsanpin-inspired bicyclic peptide **4** (non-threaded) that shows encouraging lasso peptide-like thermal and protease stability properties.²⁰ Like the reported bioactivity of sungsanpin **2a**, the bicyclic variant **4** (at 100 μ M concentration) decreased cancer cell motility as evaluated by transwell tumor cell migration and invasion assays using A549 lung carcinoma epithelial cells. However, comparison to sungsanpin **2a** and its non-threaded isomer, Sun-**2b**, were not conducted. Recently, Zou and coworkers compared the A549 cell invasion inhibitory activities of Sun-**2b** with the acyclic and head-to-tail cyclic peptides constructed from the loop-tail regions of sungsanpin-**2a**.²¹ These results were unknown at the onset of our studies and did not include any comparison to the natural lasso sungsanpin **2a**. We reasoned that time-lapse cell motility imaging assays with H1299 human non-small cell lung carcinoma cells, shown by one of our groups to exhibit faster *in vitro* motion than A549 cells, could better inform the relationship of sequence arrangement to activity for the lasso motif compared a series of Sun-**2b/2c** and Uln-**3b/3c** lasso peptide isomers.

Results and Discussion

Chemical synthesis of Sun and Uln lasso peptide isomers

To evaluate these relationships across a series of Sun/Uln-lasso peptide isomers, we developed solid-phase peptide synthesis (SPPS) strategies to access acyclic (**2d/3d**, control peptides), as well as branched cyclic (**2b/3b**), and macrocyclic (**2c/3c**) variants. We recognized that some key synthetic residues would enable modular access to the cyclic variants in this series (**Fig. 3**). All target peptides were prepared by automated, Fmoc-based solid phase peptide synthesis techniques using a 2-chlorotriptyl chloride (2-CTC)-based linker and solid support to attach the peptide to a carboxylic acid moiety. Synthetic resin-bound peptides were cleaved and globally deprotected using acidic conditions. Crude peptides were purified using reverse-phase high-performance liquid chromatography (rpHPLC).

Synthesis of acyclic peptides Sun-**2d** and Uln-**2d**

Initial efforts to prepare acyclic peptides, Sun-**2d** and Uln-**3d**, using the standard incorporation of Fmoc-Asp(Ot-Bu)-OH at respective Asp8 positions were challenged by aspartimide formation which gave inseparable mixtures. This frequently encountered issue prompted the application of strategies to avoid aspartimide formation. To prepare Sun-**2d**, we incorporated a pseudoproline dipeptide at Asp8Ser9 using commercial Fmoc-Asp(Ot-Bu)-Ser[ψ (Me,Me)Pro]-OH (**Fig. 3A**, **SI pg. S-12**). Fortunately, this strategy also improved subsequent coupling efficiencies and provided Sun-**2d** in 40% overall yield following purification by rpHPLC. Because target Uln-**3d** lacks a Ser9 or Thr9 residue needed to use the same pseudoproline dipeptide approach, we applied the cyanosulfurylide (CSY) strategy recently developed by Bode and coworkers.²² This strategy temporarily masks the requisite carboxylic acid functionality at Asp8, and unlike conventionally used sterically encumbered ester derivatives (*e.g.*, Asp(Ompe)), avoids the potential for aspartimide formation all

together. As described, we found that Fmoc-Asp(CSY)-OH **S-3** is readily prepared (**SI Scheme S-1**). And incorporated using Fmoc-based SPPS to access an Asp8(CSY)-containing peptide (**Fig. 3A**, **SI pg. S-14**) following acid-promoted cleavage and deprotection. Treatment with *N*-chlorosuccinimide (NCS) readily converts the CSY moiety at position 8 into a carboxylic acid, providing target Uln-**3d**. Although we observed a few overoxidation products, that likely derive from oxidation at Trp11, we were able to obtain Uln-**3d** in 14% overall yield following purification by rpHPLC. Next, we set out to prepare the branched cyclic lasso peptide isomers, Sun-**2b** and Uln-**3b**.

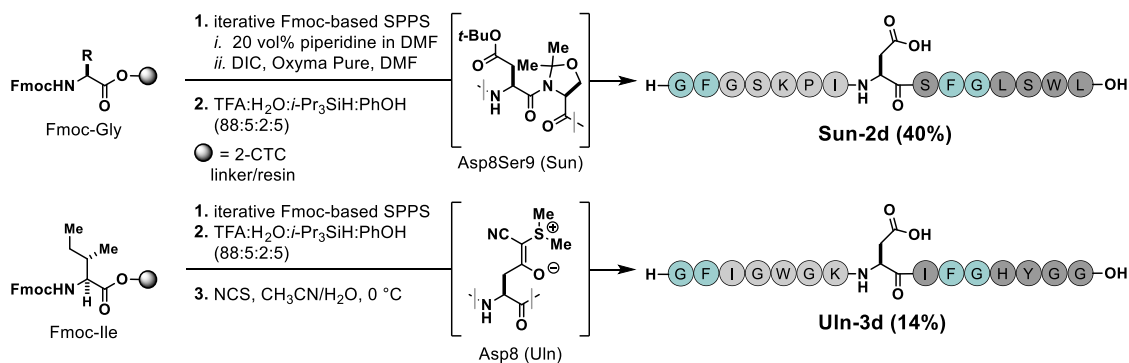
Synthesis of branched-cyclic lasso peptide isomers, Sun-**2b** and Uln-**3b**

Toward Sun-**2b** and Uln-**3b**, we developed on-resin cyclization strategies to minimize required purification events (**Fig. 3B**). Generally, strategies to prepare branched cyclic peptides leverage orthogonal protection strategies to permit *N*-terminal-selective cyclization at a carboxylic acid-containing residue sidechain. Informed by the potential for aspartimide formation at Asp8 in each sequence, we avoided the conventional strategy that would use an Asp8(Oall) residue. We recognized that most lasso peptides, including sungsanpin and ulleungdin, have a Xaa#(Gly1) isopeptide linkage, where Xaa = Asp or Glu, and # = 7-9.^{3a} Accordingly, we designed novel dipeptide **5** (Fmoc-Asp(Gly(Oall))-OH) that incorporates the Asp8(Gly1) linkage at an early stage. The coupling of H-Gly-Oall **S-5** and Fmoc-Asp(Opfp)-OtBu **S-6** (**SI Scheme S-2**), followed by deprotection of the resultant dipeptide provides Fmoc-Asp(Gly(Oall))-OH **5** in 94% isolated yield (**SI pg. S-10**). Dipeptide **5** is then readily incorporated using standard Fmoc-based SPPS techniques. Sequence elongation, on-resin deallylation and cyclization, followed by resin cleavage and global deprotection provides Sun-**2b** and Uln-**3b** in 6% and 15% overall yields, respectively. We found this strategy to circumvent aspartimide formation and enable streamlined access to branched cyclic lasso peptide isomers, Sun-**2b** and Uln-**3b**. Given the efficient preparation and utility of dipeptide **5** for on-resin peptide cyclization, other branched cyclic lasso peptide isomers should be accessible with this method. Next, we set out to prepare the macrocyclic lasso peptide isomers, Sun-**2c** and Uln-**3c**.

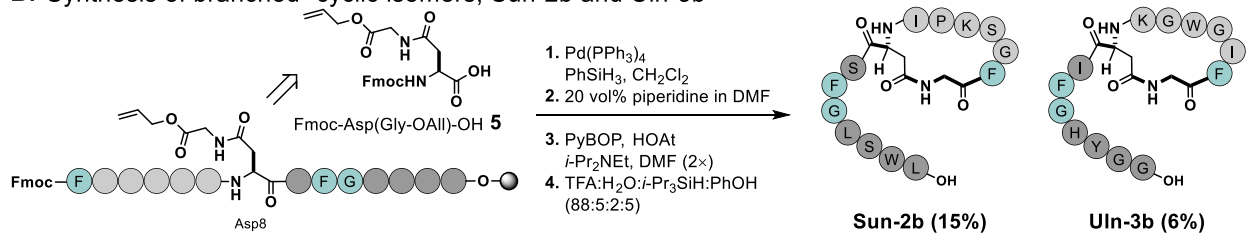
Synthesis of macro-cyclic lasso peptide isomers, Sun-**2c** and Uln-**2c**

In general, the head-to-tail cyclization of peptides can be especially challenging. Large ring-forming cyclizations incur many entropic penalties during backbone preorganization.²³ Solution-phase cyclization strategies often leverage high dilution or pseudo high dilution conditions to minimize oligomerization. However, such approaches can be met with epimerization and hydrolysis at the activated residue. We first considered chemoselective ligation approaches, such as the use of an Ala or native chemical ligation strategy which has been demonstrated for the preparation of MccJ25-**1c**.^{11,24} However, both sungsanpin and ulleungdin sequences lack Ala residues, and we sought a modular strategy that could be applied toward both Sun-**2c** and Uln-**3c**. We recognized that the Asp8 residue common to targets Sun-**2c** and Uln-**3c** could serve as a sidechain anchoring point (**Fig. 3C**). Unsurprisingly, attempts to cyclize sidechain anchored peptides were unsuccessful for both sequences. In response, we incorporated *N*-(2,4-dimethoxy)benzyl (Dmb) groups in hopes of inducing backbone preorganization and minimizing solid-phase

A. Synthesis of acyclic peptides, Sun-2d and Uln-3d



B. Synthesis of branched- cyclic isomers, Sun-2b and Uln-3b



C. Synthesis of macro- cyclic isomers, Sun-2c and Uln-3c

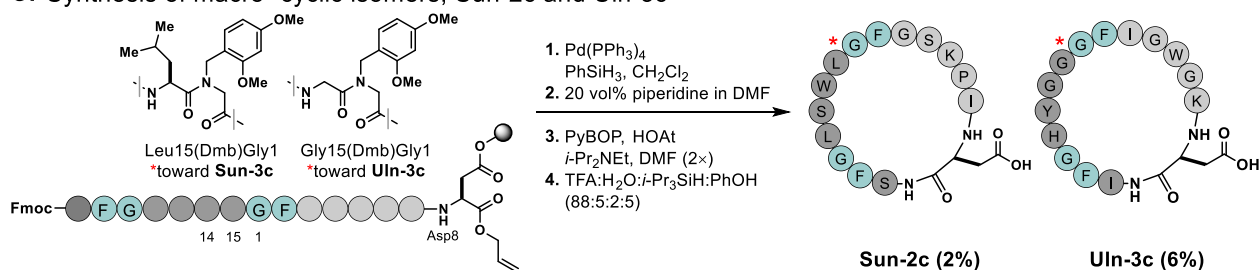


Figure 3. On-resin strategies for the synthesis of acyclic (Sun-2d and Uln-3d), branched-cyclic (Sun-2b and Uln-3b), and macrocyclic variants (Sun-2c and Uln-3c) of sungsanpin and ulleungdin lasso peptides.

aggregation to favor macrocyclization.²⁵ In each series, we found the incorporation of Dmb groups, using Fmoc-Leu15(Dmb)Gly1-OH for Sun-2c and Fmoc-Gly15(Dmb)Gly1-OH for Uln-3c (Fig. 3C, SI pgs. S-20 and S-22, respectively), enabled successful macrocyclizations to afford Sun-2c and Uln-3c in 2% and 6% overall yields, respectively, following resin cleavage, global deprotection, and purification by rpHPLC.

Characterization studies

Characterization using MS/MS

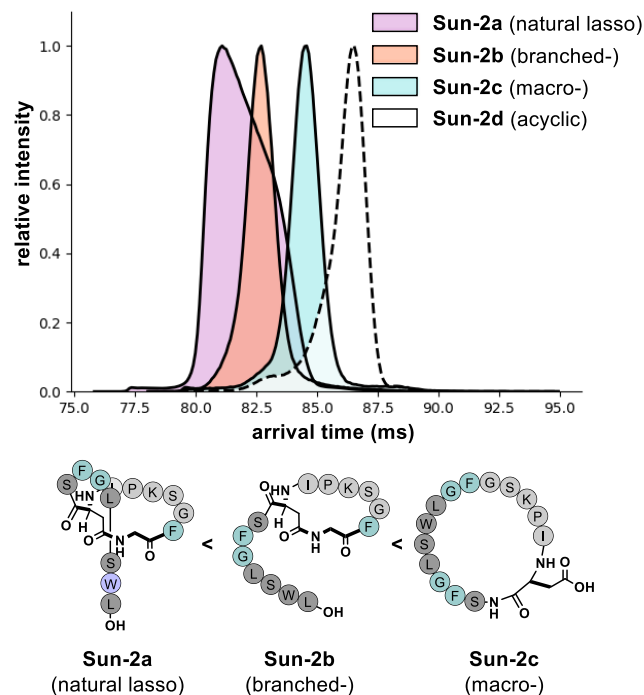
To evaluate purity and identify, we first characterized synthetic variants in the series using analytical LCMS monitored by UV with $\lambda_{\max} = 220$ nm (see the SI). Next, each variant was characterized using tandem mass spectrometry, MS/MS. Interestingly, while sungsanpin and ulleungdin peptides share only one-third sequence homology, their molecular weights are almost identical. For example, the synthetic acyclic peptides, Sun-2d and Uln-3d, have calculated $[M+H]^+$ ions = 1610.8 m/z . Although we know sequence because of how the peptides were prepared, MS/MS analysis provides data to confirm connectivity. As expected, both Sun-2d and Uln-3d displayed the indicative b and y ions associated

with fragmentation of their selected $[M+2H]^{2+}$ ions ($m/z = 806$). For branched cyclic isomers, Sun-2b and Uln-3b, we observed fragmentation patterns common to previously reported branched cyclic peptides.^{26,27} The MS/MS spectra for Sun-2b and Uln-3b, with selection for $[M+2H]^{2+}$ parent ions ($m/z = 797$), showed key tail-localized fragmentation resulting in daughter ions with preservation of the branched cyclic (ring) features. The MS/MS spectra for macrocyclic isomers, Sun-2c and Uln-3c, with selection for $[M+2H]^{2+}$ parent ions ($m/z = 797$), showed fragmentation patterns that importantly confirmed the synthetically installed Asp8Ser9 and Asp8Ile9 linkages, respectively.

Traveling wave ion mobility spectrometry-mass spectrometry

Ion mobility spectrometry-mass spectrometry is used to separate isobaric ions based on their size, shape, and charge. We turned to traveling wave ion mobility spectrometry (TWIMS) performed on the commercially available Waters Cyclic IMS-MS platform to learn more about the shape of synthetic isomers in the sungsanpin and ulleungdin series (Fig. 4). We selected for the $[M+2H]^+$ ion across each series, and the

A. Sungsanpin series: $[M+2H]^{2+}$



B. Ulleungdin series: $[M+2H]^{2+}$

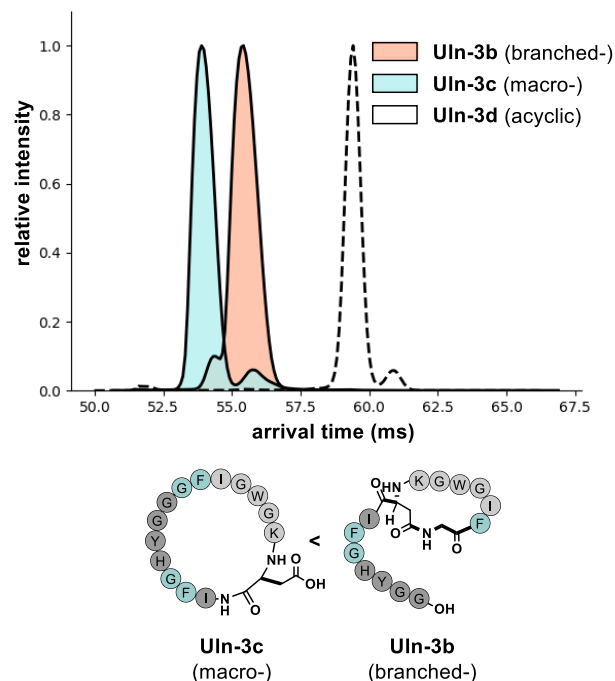


Figure 4. 8 m (A) and 5 m (B) cIMS-MS separations differentiates lassoed-, branched-, and macrocyclic peptide isomers.

relative intensity was normalized based on the highest acquired intensity measurement.

As anticipated, natural sungsanpin **2a** exhibited the earliest arrival time ($t_a = 81.0$ ms, highest mobility), which can be attributed to its compact threaded shape (Fig. 4A). Interestingly, **2a** also showed a wider peak shape relative to

branched Sun-**2b** ($t_a = 82.8$ ms) and macrocyclic Sun-**2c** ($t_a = 84.3$ ms) isomers, which suggests that additional conformations may be accessible in the gas phase. For reference, acyclic Sun-**2d** isomer ($t_a = 86.6$ ms) had the latest arrival, consistent with its higher degree of rotational freedom relative to lassoed and cyclic peptide variants. Interestingly, the study reported by Tulla-Puche and coworkers suggested that accessible sidechain-based electrostatic interactions may further stabilize (constrain) the dominant conformation for sungsanpin **2a** in the gas phase.²⁰ The ability of branched Sun-**2b** and bicyclic **4** variants to access similar sidechain-based electrostatic interactions may explain why their arrival time distributions are more lasso-like (closest in arrival time) than the macrocyclic isomer, Sun-**2c**. In the ulleungdin series, the macrocyclic Uln-**3c** isomer ($t_a = 54.0$ ms) arrives before the branched Uln-**3b** isomer ($t_a = 55.5$ ms), followed by the acyclic isomer, Uln-**3d** ($t_a = 59.4$ ms) (Fig. 4B). This surprising swap in arrival time suggests that Uln-**3c** (macrocyclic) can adopt a more compact conformation than Uln-**3b** (branched). The comparison of arrival times within a series showed informative trends. As anticipated, non-threaded cyclic peptides arrive later than their lassoed isomer. The analysis of $[M+2H]^+$ ions across series shows a difference in average arrival time (Sun series: avg $t_a = \sim 83$ ms vs. Uln series: avg $t_a = \sim 56$ ms) attributable to sequence differences that shift their respective mobilities (*i.e.*, size/shape).

Biological activity

Previous reports from one of our groups, and the Ahn group, independently showed that sungsanpin **2a** and ulleungdin **3b** at 50 μ M concentration inhibit 47% and 48% of A549 lung carcinoma epithelial cells, respectively, from invading the lower chamber in a transwell invasion assay.^{18,19} Based on the hypothesis that the native lasso motif provides beneficial preorganization to the conserved residues in the sequence, we evaluated the series of synthetic accessible Sun and Uln isomers using time-lapse cell imaging-based cancer cell migration assays to track individual cells and globally determine relationship of sequence arrangement to this activity. Prior to the migration assays, proliferation assays were run at 25 μ M and 50 μ M concentration for each peptide over a 24-hour period to confirm cell viability and proliferation relative to the untreated control (DMSO) (SI Fig. S-58). The cells were labeled with Janus green dye to measure the number of viable cells (absorbance at 620 nm) present after 24 hours. When compared against cells treated with synthetic isomers, the cells treated with sungsanpin **2a** exhibited the lowest number of proliferated cells, at 25 μ M and 50 μ M. More cells were observed for the 25 μ M **2a** vs. 50 μ M **2a** treatments. Therefore, we chose the 25 μ M concentration for subsequent time-lapse cell imaging studies. Imaging the cells over the course of 15 h and again after 24 h of 25 μ M **2a** showed that the cells are viable with the treatment (SI Fig. S-59-64).

Previously, one of our groups showed that H1299 human non-small cell lung carcinoma cells exhibit faster *in vitro* motion than A549 cells, and accordingly, migration assays using H1299 cells can provide a better measure on substrate inhibitory effects.²⁸ Therefore, we chose to use H1299 cells in time lapse cell imaging experiments. For all experiments, cell nuclei were labeled with DRAQ5TM for automated tracking via a MATLAB workflow using custom software based on u-track multiple particle tracking. Only cells that displayed persistent

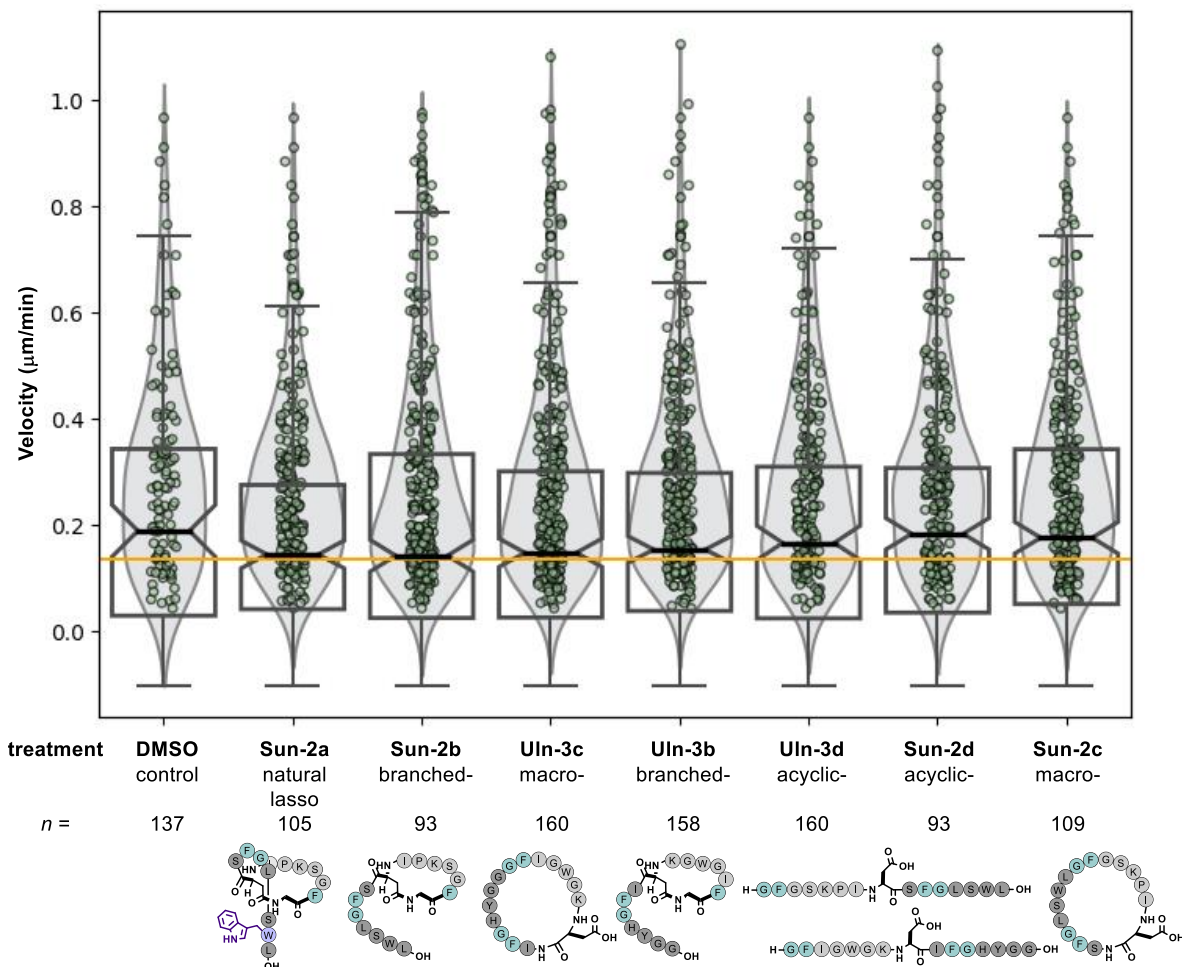


Figure 5 Natural lasso, branched cyclic, and macrocyclic peptides exhibit better migration inhibition than acyclic or Sun-2c macro peptides

random walk were included in the velocity calculations. Velocity was calculated as mean squared displacement (MSD).

In our results, we applied a p-value of 0.1 as significant, meaning there is a 10% chance the samples are drawn from the same distribution. The median velocity of cells treated with sungsanpin **2a** was lower than control cells (**Fig. 5** & **SI Table S-1**, lasso **2a** median velocity = 0.23 $\mu\text{m}/\text{min}$ vs DMSO velocity = 0.28 $\mu\text{m}/\text{min}$, $p = 0.08$). Similarly, the velocity of cells treated with branched Sun-**2b** was lower than control cells (branched Sun **2b** median velocity = 0.21 $\mu\text{m}/\text{min}$ vs. DMSO velocity = 0.28 $\mu\text{m}/\text{min}$, $p = 0.08$). Thus, cell migration may be inhibited by treatments, **2a** or Sun-**2b**, in H1299 cancer cells. Branched Uln-**3b** (MSD velocity = 0.23 $\mu\text{m}/\text{min}$) and macrocyclic Uln-**3c** (MSD velocity = 0.22 $\mu\text{m}/\text{min}$) isomers also exhibit a lower trending MSD velocity in comparison with control cells (DMSO treatment, MSD velocity = 0.28 $\mu\text{m}/\text{min}$, p -values = 0.15). Finally, at p-values greater than 0.40, we find that treatment with acyclic Sun-**2d** (MSD velocity = 0.27 $\mu\text{m}/\text{min}$, $p = 0.43$), acyclic Uln-**3d** (MSD velocity = 0.23 $\mu\text{m}/\text{min}$, $p = 0.42$), and macrocyclic Sun-**2c** (MSD velocity = 0.25 $\mu\text{m}/\text{min}$, $p = 0.60$) did not slow migration.

We suggest that three of the four constrained synthetic isomers, branched Sun-**2b**, branched Uln-**3b**, and macrocyclic Uln-**3c** isomers, can slow the migration of H1299 cancer cells, as interpreted by analyses of their MSD velocities. The

macrocyclic Sun-**3c** isomer, and as anticipated, the more flexible acyclic variants, Sun-**2d** and Uln-**3d**, did not slow cell migration. Interestingly, the relative trend of median velocities in the sungsanpin series (**2a** \geq **2b** > **2c** > **2d**) qualitatively tracks well with the TWIMS arrival times (**Fig. 4A**). This was also observed for the ulleungdin series (**3c** > **3b** > **3d**), where the Uln-**3c** and Uln-**3b** swap is seen in both TWIMS arrival time and median velocities (**Fig. 4B**). This suggests that the more compact isomers could exhibit a higher degree of preorganization. However, more in-depth experiments would be needed to determine the extent of solution-based conformational similarity between the conserved residues for each series to corroborate this observation. Additionally, future stability experiments could decouple the lack of observed activity and the susceptibility of each isomer toward proteolytic degradation.²⁰ This might be especially informative for the macrocyclic Sun-**2c**, which was less compact despite being constrained, and could make it more susceptible to degradation leading to no indication of slowed migration in H1299 cells. Taken together, we observe a complex interplay between the conserved sequence and shape using time-lapse cell imaging assays to monitor H1299 cell displacement as an improved readout for cancer cell migration inhibition.

Conclusion

The appreciation for lasso peptides as stable and highly constrained scaffolds with promising biological activities inspired our efforts to evaluate the relationship of conserved residue arrangement and activity across synthetically accessible lasso peptide isomers of sungsanpin **2a** and ulleungdin **3a**. We identified Asp8 as a common residue that can be strategically modified to access acyclic, branched, and macrocyclic isomers in both the sungsanpin and ulleungdin series. Access to these isomers enabled a systematic and broad understanding of lasso peptide structure as it relates to the inhibition of cancer cell migration for these peptide sequences. Our results suggest that constrained lasso peptide isomers, Sun-**2b**, Uln-**3b**, and Uln-**3c**, exhibit an ability to slow H1299 cell migration comparable to natural sungsanpin **2a**. Our results, and those reported by Zou and coworkers,²¹ suggest that the lasso motif is not a required feature to slow cancer cell migration. These lasso peptide isomers, Sun-**2b**, Uln-**3b**, and Uln-**3c** may serve as a useful synthetically accessible lead compounds for projected modeling, target identification, and optimization studies, which could inform the future design of these constrained peptides.

ASSOCIATED CONTENT

Supporting Information

The Supporting Information is available free of charge at [_____](#). Experimental procedures and characterization data for all synthetic peptides, analytical characterization, and details of the biological cellular assays (PDF).

AUTHOR INFORMATION

Corresponding Author

Andrew G. Roberts –

Department of Chemistry, University of Utah, Salt Lake City, Utah 84112, United States; orcid.org/0000-0002-2221-534X; email: roberts@chem.utah.edu

Notes

The authors declare no competing financial interests.

ACKNOWLEDGMENT

We are grateful for financial support from the University of Utah, Department of Chemistry. We thank the ALSAM Foundation for supporting the summer research internship for Mark A. Stevens. We acknowledge the Cell Imaging Core at the University of Utah for use of the Nikon Automated Widefield Microscope and thank Dr. Xiang Wang and Mike Bridge for their assistance. We would like to thank Rebecca Zitnay and Akib Khan from the Mendoza laboratory for helpful discussions and assistance with time lapse cell imaging experiments. We are grateful to Karsten Eastman from the Bandarian laboratory at the University of Utah for assistance with MS/MS data acquisition. Additionally, we thank Dr. Hsiaonung Chen from the Mass Spectrometry Facility at the University of Utah for assistance with LC-MS, HRMS, and MS/MS data acquisition. Finally, we would like to thank Dr. Jordan Dotson and Brittany Haas from the Sigman laboratory for assistance with CD spectroscopy and UPLC-MS instrumentation and data acquisition, respectively. NMR spectroscopy results included in this report were recorded at the David M. Grant NMR Center, a University of Utah Core Facility. Funds for construction of this

center and the helium recover system were obtained from the University of Utah and the National Institutes of Health (NIH) awards 1C06RR017539-01A1 and 3R01GM063540-17W1, respectively. NMR instruments were purchased with support of the University of Utah and the NIH award 1S100D25241-01.

REFERENCES

- (1) Hegemann, J. D.; Zimmermann, M.; Xie, X.; Marahiel, M. A. Lasso Peptides: An Intriguing Class of Bacterial Natural Products. *Acc. Chem. Res.* **2015**, *48* (7), 1909–1919.
- (2) Pan, S. J.; Link, A. J. Sequence Diversity in the Lasso Peptide Framework: Discovery of Functional Microcin J25 Variants with Multiple Amino Acid Substitutions. *J. Am. Chem. Soc.* **2011**, *133* (13), 5016–5023.
- (3) a) Tietz, J. I.; Schwalen, C. J.; Patel, P. S.; Maxson, T.; Blair, P. M.; Tai, H.-C.; Zakai, U. I.; Mitchell, D. A. A New Genome-Mining Tool Redefines the Lasso Peptide Biosynthetic Landscape. *Nat. Chem. Biol.* **2017**, *13* (5), 470–478. b) Maksimov, M. O.; Link, A. J. Prospecting Genomes for Lasso Peptides. *J. Ind. Microbiol. Biotechnol.* **2014**, *41* (2), 333–344.
- (4) Hegemann, J. D.; Zimmermann, M.; Zhu, S.; Klug, D.; Marahiel, M. A. Lasso Peptides from Proteobacteria: Genome Mining Employing Heterologous Expression and Mass Spectrometry. *Pept. Sci.* **2013**, *100* (5), 527–542.
- (5) Mevaere, J.; Goulard, C.; Schneider, O.; Sekurova, O. N.; Ma, H.; Zirah, S.; Afonso, C.; Rebuffat, S.; Zotchev, S. B.; Li, Y. An Orthogonal System for Heterologous Expression of Actinobacterial Lasso Peptides in *Streptomyces* Hosts. *Sci. Rep.* **2018**, *8* (1), 8232.
- (6) Si, Y.; Kretsch, A. M.; Daigh, L. M.; Burk, M. J.; Mitchell, D. A. Cell-Free Biosynthesis to Evaluate Lasso Peptide Formation and Enzyme-Substrate Tolerance. *J. Am. Chem. Soc.* **2021**, *143* (15), 5917–5927.
- (7) Liu, T.; Ma, X.; Yu, J.; Yang, W.; Wang, G.; Wang, Z.; Ge, Y.; Song, J.; Han, H.; Zhang, W.; Yang, D.; Liu, X.; Ma, M. Rational Generation of Lasso Peptides Based on Biosynthetic Gene Mutations and Site-Selective Chemical Modifications. *Chem. Sci.* **2021**, *12* (37), 12353–12364.
- (8) Knappe, T. A.; Manzenrieder, F.; Mas-Moruno, C.; Linne, U.; Sasse, F.; Kessler, H.; Xie, X.; Marahiel, M. A. Introducing Lasso Peptides as Molecular Scaffolds for Drug Design: Engineering of an Integrin Antagonist. *Angew. Chem. Int. Ed.* **2011**, *50*, 8714–8717.
- (9) Chen, M.; Wang, S.; Yu, X. Cryptand-Imidazolium Supported Total Synthesis of the Lasso Peptide BI-32169 and Its D-Enantiomer. *Chem. Commun.* **2019**, *55* (23), 3323–3326.
- (10) a) Saito, F.; Bode, J. W. Synthesis and Stabilities of Peptide-Based [1]Rotaxanes: Molecular Grafting onto Lasso Peptide Scaffolds. *Chem. Sci.* **2017**, *8* (4), 2878–2884. b) Young, M. J.; Akien, G. R.; Evans, N. H. An amide hydrogen bond templated [1]rotaxane displaying a peptide motif – demonstrating an expedient route to synthetic mimics of lasso peptides. *Org. Biomol. Chem.* **2020**, *18*, 5203–5209.
- (11) Wilson, K. A.; Kalkum, M.; Ottesen, J.; Yuzenkova, J.; Chait, B. T.; Landick, R.; Muir, T.; Severinov, K.; Darst, S. A. Structure of Microcin J25, a Peptide Inhibitor of Bacterial RNA Polymerase, is a Lassoed Tail. *J. Am. Chem. Soc.* **2003**, *125* (41), 12475–12483.
- (12) Soudy, R.; Wang, L.; Kaur, K. Synthetic Peptides Derived from the Sequence of a Lasso Peptide Microcin J25 Show Antibacterial Activity. *Bioorg. Med. Chem.* **2012**, *20* (5), 1794–1800.
- (13) Hammami, R.; Bédard, F.; Gomaa, A.; Subirade, M.; Biron, E.; Fliss, I. Lasso-inspired peptides with distinct antibacterial mechanisms. *Amino Acids* **2015**, *47*, 417–428.
- (14) Braffman, N. R.; Piscottab, F. J.; Hauvera, J.; Campbella, E. A.; Link, A. J.; Darst, S. A. Structural mechanism of transcription inhibition by lasso peptides microcin J25 and capistrain. *Proc. Natl. Acad. Sci.* **2019**, *116* (4), 1273–1278.
- (15) Katahira, R.; Shibata, K.; Yamasaki, M.; Matsuda, Y.; Yoshida, M. RES-701-1, comparative study of the synthetic and the microbial-origin compounds. *Bioorg. & Med. Chem. Lett.* **1995**, *5* (15), 1595–1600.
- (16) a) Shibata, K.; Suzawa, T.; Ohno, T.; Yamada, K.; Tanaka, T.; Tsukuda, E.; Matsuda, Y.; Yamasaki, M. Hybrid Peptides Constructed from RES-701-1, an Endothelin B Receptor Antagonist, and Endothelin; Binding Selectivity for Endothelin Receptors and Their Pharmacological Activity. *Bioorg. Med. Chem.* **1998**, *6* (12), 2459–2467. b) Suzawa, T.; Shibata, K.; Tanaka, T.; Matsuda, Y.; Yamasaki, M.

RES-701-1/Endothelin hybrid peptide having a potent binding activity for type B receptor. *Bioorg. & Med. Chem. Lett.* **1997**, *7* (13), 1715–1720.

(17) Fares, J.; Fares, M. Y.; 4, Khachfe, H. H.; Salhab, H. A.; Fares, Y. Molecular principles of metastasis: a hallmark of cancer. *Signal Transduction and Targeted Therapy.* **2020**, *5*:28.

(18) Um, S.; Kim, Y.-J.; Kwon, H.; Wen, H.; Kim, S.-H.; Kwon, H. C.; Park, S.; Shin, J.; Oh, D.-C. Sungsanpin, a Lasso Peptide from a Deep-Sea Streptomycete. *J. Nat. Prod.* **2013**, *76* (5), 873–879.

(19) Son, S.; Jang, M.; Lee, B.; Hong, Y.; Ko, S.; Jang, J.; Ahn, J. S. Ulleungdin, a Lasso Peptide with Cancer Cell Migration Inhibitory Activity Discovered by the Genome Mining Approach. *J. Nat. Prod.* **2018**, *81* (10), 2205–2211.

(20) Martin-Gómez, H.; Albericio, F.; Tulla-Puche, J. A Lasso-Inspired Bicyclic Peptide: Synthesis, Structure and Properties. *Chem. Eur. J.* **2018**, *24* (72), 19250–19257.

(21) Li, A.; Zou, J.; Zhuo, X.; Chen, S.; Chai, X.; Gai, C.; Li, X.; Zhao, Q.; Zou, Y. Rational Optimizations of the Marine-Derived Peptide Sungsanpin as Novel Inhibitors of Cell Invasion. *Chem. Biodiversity.* **2023**, *20* (2), e202201221.

(22) Neumann, K.; Farnung, J.; Baldauf, S.; Bode, J. W. Prevention of Aspartimide Formation during Peptide Synthesis Using Cyanosulfurylides as Carboxylic Acid-Protecting Groups. *Nat. Commun.* **2020**, *11*:982.

(23) Girvin, Z. C.; Andrews, M. K.; Liu, X.; Gellman, S. H. Foldamer-

templated catalysis of macrocycle formation. *Science.* **2019**, *366* (6472), 1528–1531.

(24) Rosengren, K. J.; Clark, R. J.; Daly, N. L.; Goransson, U.; Jones, A.; Craik, D. J. Microcin J25 Has a Threaded Sidechain-to-Backbone Ring Structure and Not a Head-to-Tail Cyclized Backbone. *J. Am. Chem. Soc.* **2003**, *125* (41), 12464–12474.

(25) Rosengren, K. J.; A. R.; Morejón, M. C.; Rivera, D. G.; Wessjohann, L. A. Peptide Macrocyclization Assisted by Traceless Turn Inducers Derived from Ugi Peptide Ligation with Cleavable and Resin-Linked Amines. *Org. Lett.* **2017**, *19* (15), 4022–4025.

(26) Dit Fouque, K. J.; Moreno, J.; Hegemann, J. D.; Zirah, S.; Rebuffat, S.; Fernandez-Lima, F. Identification of Lasso Peptide Topologies Using Native Nano electrospray Ionization-Trapped Ion Mobility Spectrometry–Mass Spectrometry. *Anal. Chem.* **2018**, *90* (8), 5139–5146.

(27) Jeanne Dit Fouque, K.; Bisram, V.; Hegemann, J. D.; Zirah, S.; Rebuffat, S.; Fernandez-Lima, F. Structural Signatures of the Class III Lasso Peptide BI-32169 and the Branched-Cyclic Topoisomers Using Trapped Ion Mobility Spectrometry–Mass Spectrometry and Tandem Mass Spectrometry. *Anal. Bioanal. Chem.* **2019**, *411* (24), 6287–6296.

(28) Ingram, K.; Samson, S. C.; Zewdu, R.; Zitnay, R. G.; Snyder, E. L.; Mendoza, M. C. NKX2-1 Controls Lung Cancer Progression by Inducing DUSP6 to Dampen ERK Activity. *Oncogene* **2022**, *41* (2), 293–300.